

# On regime transitions in contact-based social contagion models on multiplex networks

Author: Joan Hernández Tey.

*Facultat de Física, Universitat de Barcelona, Diagonal 645, 08028 Barcelona, Spain.*

Advisor: Emanuele Cozzo

In this paper, we study regime transitions on a general epidemiclike social contagion model on a multiplex system. We first examine layer-localisation to delocalisation transition analysing the inverse participation ratio (IPR) for the different layers of the system. In addition, we develop a perturbation analysis to obtain a new analytical approximation for the transition point and an expression for the non dominant layer IPR on the localised regime. Furthermore, we study a nondominant to dominant regime transition and obtain an analytical expression for the transition point on a random regular network and an approximation for an Erdős-Rényi network. We further analyse this transitions with dynamical simulations using a Quasi-stationary algorithm.

## I. INTRODUCTION

Social media sites have recently become one of the most common sources of information. However, a lot of the information on these online social platforms is usually incorrect. There are a large number of people who try to create fake news. For example, a false rumour about Stephen Hawking saying that "aliens existed on the far land of the moon" [1]. Therefore, it is no surprise that there is strong interest in modelling this systems.

Social contagion processes depend on many factors, such as the structure of the network's topology and the dynamics of information spreading.

Individuals in this networks can have complex states [2] however, the simplest systems only have two states, susceptible/inactive if they are not transmitting information and infected/active if they are (SIS). For instance, people using a hashtag in Twitter can be our infected/active individuals, and their followers are susceptible and may be infected. From a dynamical point of view, these are stochastic processes that depend on the contacts and tend to a certain stationary state and it presents a phase transition when this state changes from being an inactive state (microscopic fraction of infected individuals) to an active state (macroscopic fraction of infected individuals).

However, the advent of new communication platforms and their rising popularity have made modelling social contagion networks more complex. Individuals are constantly exposed to different sources of information which they do not value equally. This directly affects the structure and the dynamics of the systems and adds a whole other dimension to the study. For this reason we need to study multiplex systems [3, 4] which are used to represent complex systems that are composed of other subsystems. These systems are divided into layers with a coupling parameter between them and each one represents different social media platforms. This adds a new localization feature, this means that the stationary state can now be found in a layer (localised) or be found everywhere (delocalised).

To model these kinds of networks, complex theory

physics uses graphs to represent social websites. Graphs consist of nodes interconnected with their neighbours. In this paper, we study two types of graphs: Random Regular graphs (RR) where all of the nodes have the same number of neighbours  $k$  and Erdős-Rényi graphs (ER) where nodes have a Binomial distribution of neighbours around  $\langle k \rangle$ . We can represent a graph as an adjacency matrix ( $A$ ). It is a matrix where each  $A_{ij}$  is one if node  $i$  and  $j$  are connected. Furthermore, we add weight to these values to set a probability of contact. Two common models are fully reactive model (FR) and contact process model (CP). FR models have a probability of contact equal to one therefore all neighbours are contacted in each time-step. CP models have a probability of contact  $k^{-1}$  thus one neighbour is contacted in each time step.

The study of the structure of networks was already important due to the largest eigenvalue of the network allowing us to find the critical point of the phase transition. With the addition of a multiplex system, it is even more valuable because we can now study the localisation of the stationary state analysing the leading eigenvector (eigenvector with the largest eigenvalue of the system) [5].

In network theory, the inverse participation ratio is commonly used to characterize this localization feature. It is defined as follows

$$IPR(v) = \sum_i^X v_i^4, \quad (1)$$

where  $v$  is the eigenvector with the largest eigenvalue and  $X$  is the network size. In case we have a two-layer systems where all of the nodes of layer one have their corresponding node in layer two,  $X = 2N$  ( $N$  being the number of nodes of each layer). Thus,  $IPR(v) = IPR_1(v_1) + IPR_2(v_2)$ , where  $v_1$  is the first layer part of  $v$  and  $v_2$  is the second layer part. This fact is important to see which layer is dominant (has the largest eigenvalue). The inverse participation ratio for the dominant layer behaves differently from the non-dominant one.

The inverse participation ratio analysis of a two-layer multiplex system was previously done in Ref. [5] with a fully reactive SIS model. They obtained a numerical form for the transition point between localised and delocalised regime and the  $IPR_{ND}$ . We further study this using perturbation theory on the IPR. We obtain a new analytical approximation for the latter and confirm the universal curve. Furthermore, we consider a generalization of the SIS model introduced in Ref. [3]. It adds a new parameter that controls the contact probability. We study how this new parameter affects the localization. We show that changing this parameter for just one layer creates a new transition where the non-dominant layer becomes the dominant layer. We also confirm this results with quasi stationary simulations to study the dynamical aspect for the systems.

## II. SUPRA CONTACT PROBABILITY MATRIX

Let us now define the mathematical framework where we are working on, [3]. The contact probability matrix for a monoplex network with  $N$  nodes is

$$(R)_{ij} = 1 - \left(1 - \frac{(A)_{ij}}{k_i}\right)^{\gamma_i}, \quad (2)$$

where  $A$  is the adjacency matrix for the monoplex and  $k_i$  is the number of neighbours for each node. This model interpolates two popular spreading models, fully reactive and contact process. The parameter that controls this interpolation is  $\gamma$ . When  $\gamma = 1$  the probability to contact each neighbour is  $\frac{1}{k_i}$ , this means that on average, at each time step, infected nodes contact one of their neighbours (contact process). On the contrary, when  $\gamma \rightarrow \infty$ , the probability of contacting each node is one. Therefore, each node contacts all of its neighbours at the same time (FR).

Let us generalize the monoplex probability matrix to a multiplex system made with  $N$  nodes and  $M$  layers. In this scenario we have  $R_\alpha = R$  for each layer where each variables  $A$ ,  $\vec{K}$  and  $\gamma$  can be different. Then, the multiplex supracontact matrix is

$$\bar{R} = \bigoplus_{\alpha} R_{\alpha} + pC, \quad (3)$$

where the first part is direct sum of each layer contact probability matrix and  $C$  is a matrix where  $C_{ij} = 1$  if the same node is present on different layers. Therefore, the supra contact probability matrix has a block structure with  $R_\alpha$  on the diagonal and the  $C$  values out of this diagonal, for instance  $\bar{R} = \begin{pmatrix} R_1 & C_{12} \\ C_{21} & R_2 \end{pmatrix}$  for a two layer multiplex network. Furthermore, when doing the discrete time evolution equation for the contagion probability of a node  $i$  [3],

$$\begin{aligned} \vec{p}(t+1) &= [\vec{1} - \vec{p}(t)] * [\vec{1} - \vec{q}(t)] + (1 + \vec{\mu}) * \vec{p}(t) \\ &+ \vec{\mu} * [\vec{1} - \vec{q}(t)] * \vec{p}(t), \end{aligned} \quad (4)$$

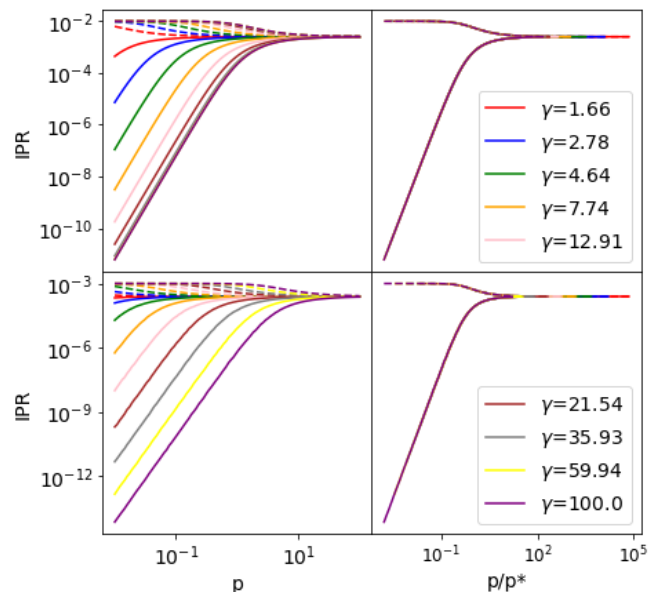


FIG. 1: The top panels are a representation of the inverse participation ratio as a function of  $p$  and  $p/p^*$ . It is a regular network with  $k_1 = 10$ ,  $k_2 = 8$  and 100 nodes. The bottom panels are also a representation of  $IPR$  as a function of  $p$  and  $p/p^*$ . It is a Erdős-Rényi network with  $\langle k_1 \rangle = 10$ ,  $\langle k_2 \rangle = 8$  and 1000 nodes. The ER networks figures have a little bit of noise.

where  $q_i(t) = \prod_j [1 - \beta R_{ij} p_j(t)]$  is the probability to not be infected for the node  $i$ , we observe that  $p = \frac{\epsilon}{\beta}$  where  $\beta$  characterizes the contagion rate within layers and  $\epsilon$  characterizes the contagion probability between the same node in different layers. Another relevant parameter is  $\mu$  which is the probability of an active state decaying to an inactive one. This parameter is important because when solving the stationary state of (4) we obtain that the inactive-active phase transition point is  $\left(\frac{\beta}{\mu}\right)_c = \frac{1}{\Lambda_{max}}$  [3].

## III. PERTURBATIVE ANALYSIS

In this section, we study localisation properties using perturbation approximation on the inverse participation ratio to obtain the characterising value of the localised-delocalized regime transition  $p^*$ . This is a demonstration considering a RR network but later we see that it is a good approximation for an ER graph.

The analytical expression for  $IPR_2$  is derivable using perturbation theory. Let us consider  $p \ll 1$ , then in  $\bar{R} = \bigoplus_{\alpha} R_{\alpha} + pC$ , the  $p$  dependant part can be studied as a perturbation. Therefore  $\bar{\Lambda} \approx \Lambda_0 + p\Delta\Lambda$  and  $\vec{v} \approx \vec{v}_0 + p\Delta\vec{v}$ .

In addition, as  $R = \bigoplus_{\alpha} R_{\alpha}$  is a diagonal block matrix, its eigenvalues are the same as  $R_{\alpha}$ . Before using perturbation theory, it is important to analyse the eigenvector with the biggest eigenvalue. As we are considering a 2-

layer system, one layer dominates because it has a bigger eigenvalue (we consider the first one for the explanation). Let us assume a RR network, the largest eigenvalue of each layer is  $\Lambda_\alpha = k_\alpha \cdot (1 - (1 - \frac{1}{k_\alpha})^{\gamma_\alpha})$ , that's because all of  $k_\alpha$  elements in  $R_\alpha$  are positive and equal. Its corresponding eigenvector is a normalized  $\vec{1}$  because, when multiplied to any  $R_\alpha$  column, it results in  $k_\alpha$  no matter how  $R_{\alpha ij}$  is distributed.

We examine a two-layer multiplex system where the first layer is dominant. Thus,  $\Lambda_1 > \Lambda_2$  where  $\Lambda_1$  and  $\Lambda_2$  are the largest eigenvalues of layers 1 and 2. As we study a RR multiplex system its dominant eigenvector,  $\vec{v}_0$ , is  $\vec{v}_0 = \begin{pmatrix} \vec{v}_1 \\ 0 \end{pmatrix} = \frac{1}{N} \begin{pmatrix} \vec{1} \\ 0 \end{pmatrix}$ ,

The first-order approximation in perturbation theory on this vector is (considering normalized vectors)

$$\Delta\Lambda_{max} = \vec{v}_0^\top C \vec{v}_0 \quad (5)$$

$$\Delta\vec{v} = \sum_{v_0 \neq u_0} \frac{\vec{u}_0^\top C \vec{v}_0}{\Lambda_{v_0} - \Lambda_{u_0}} \vec{u}_0. \quad (6)$$

Let us study perturbations on this vector. First of all, the eigenvectors of a RR network are orthogonal to each other,  $\vec{u}^\top \vec{v} = \delta_{uv}$ . Moreover,  $C\vec{v}_0 = p\vec{m}_0$  where  $\vec{m}_0 = \frac{1}{N} \begin{pmatrix} 0 \\ \vec{1} \end{pmatrix}$  is the eigenvector, with the corresponding eigenvalue  $\Lambda_2$ . That is because we have the same nodes in both layers then, multiplying the eigenvector to C changes it from one layer to another. Thus, there is just one term in the sum in (6) that is not equal zero. Therefore,  $\Delta\Lambda = 0$  and  $\Delta\vec{v} = \frac{p}{\Lambda_1 - \Lambda_2} \vec{m}_0$ . Consequently, the resulting vector is

$$\vec{v} = \begin{pmatrix} \vec{v}_1 \\ \frac{p}{\Lambda_1 - \Lambda_2} \vec{v}_1 \end{pmatrix}. \quad (7)$$

Now, we can obtain  $p^*$  and  $IPR_2$ . Let us first obtain  $p^*$ . It is the  $p$  that characterizes the transition from localized to delocalized, which happens when  $IPR_1 \approx IPR_2$ . The inverse participation ratio depends directly of  $v_1$  and  $v_2$ , thus, we can establish that the transition occurs when  $v_1 \approx v_2 \approx \frac{p^*}{\Lambda_1 - \Lambda_2} v_1$ . Therefore,  $p^* = \Lambda_1 - \Lambda_2$

$$p^* = k_1 \left( 1 - \left( 1 - \frac{1}{k_1} \right)^{\gamma_1} \right) - k_2 \left( 1 - \left( 1 - \frac{1}{k_2} \right)^{\gamma_2} \right). \quad (8)$$

When  $p$  is scaled with  $p^*$ , the IPR for different  $\gamma$  collapse and we obtain the universal curve, see Fig. 1. Also, although these results are obtained assuming that we have a RR multiplex system, we can see in Fig. 1, although having a bit of noise due to randomness, that the IPR of Erdős-Rényi systems collapses under the  $p^*$  scaling. Therefore, we can assume that it is an accurate approximation for the expected value of  $p^*$  for a ER network.

Now, we obtain the expression for  $IPR_2$  for  $p < p^*$ . Calculating the inverse participation ratio on the latter

vector we obtain  $IPR_2 = \sum v_2^4 = \sum \frac{p}{\Lambda_1 - \Lambda_2} v_1$ , where  $v_1$  is a normalized vector of ones. The sum is trivial and results in

$$IPR_2 = \frac{1}{N} \left( \frac{p}{\Lambda_1 - \Lambda_2} \right)^4 \quad (9)$$

This result accurately describes the nondominant delocalized regime for RR graphs and ER graphs. Comparing our results with the ones given in Ref. [5], they obtained a numerical approximation form for  $IPR_2$  as follows  $\log IPR_2 = \alpha \log(p) + c_1$ . They obtained that  $\alpha \approx 4$  and  $c_1$  was dependant of the network. Comparing the previous expression with our analytical results, we see that  $\alpha = 4$  and  $c_1 = -4 \log(\Lambda_1 - \Lambda_2) - \log(N)$ .

#### IV. LOCALIZATION ANALYSIS IN PARAMETER $\gamma$

Another interesting study is how IPR behaves when changing  $\gamma$  for one layer. This parameter has a hard influence on the leading eigenvalue of the layer. In Fig. 2, we see that when  $\gamma = 1$ , the eigenvalue equals 1. Then, as  $\gamma$  grows, the eigenvalue tends to  $k_\alpha$  for a RR network. However, for an ER network, the eigenvalue has a similar behaviour but instead tends to  $k_\alpha + 1$  due to being a Poisson distribution in the large N limit, see Fig. 2. The following deduction assumes a RR network to define  $\Lambda_\alpha(\gamma_\alpha)$ .

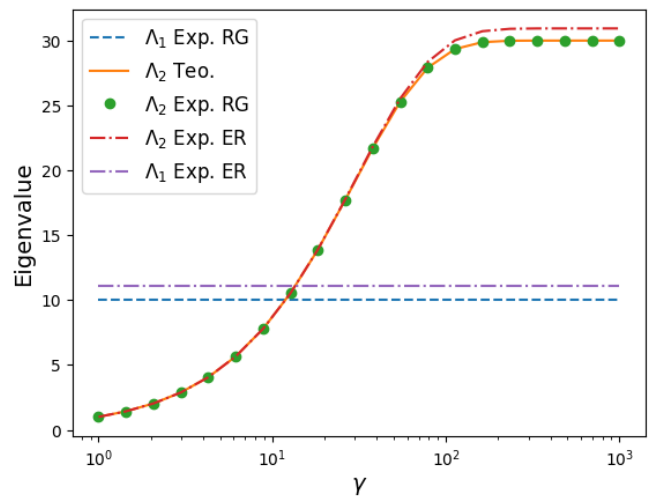


FIG. 2: Representation of the eigenvalue as a function of  $\gamma$ . In this image,  $k_1 = 10$ ,  $k_2 = 30$ , 1000 nodes and  $\gamma_1 \rightarrow \infty$ . The line is the analytical form for the leading eigenvalue of layer 2. Dots are computational eigenvalues for layer 2 with a Regular network and the dashed lines are eigenvalues for layer 1. Dot-dashed lines are eigenvalues for the Erdős-Rényi network, red for layer 2 and purple for layer 1.

Let us consider a system where the first layer has  $\gamma_1 \rightarrow \infty$  with  $k_1 = 10$  and the second has  $k_2 = 30$

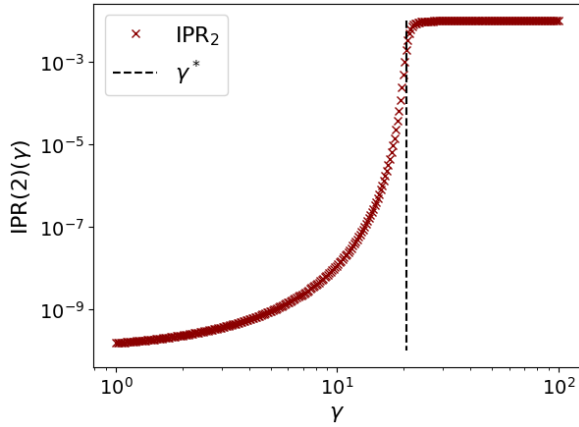


FIG. 3: Representation of  $IPR_2$  as a function of  $\gamma$  for a fixed  $p = 0.1$ . Layer 1 has a fixed value of  $\gamma \rightarrow \infty$ . Its a regular network with 100 nodes and  $k_1 = 10$  and  $k_2 = 12$ . In this network,  $\gamma^* = 20.59$

and a variable  $\gamma$ . In this scenario, for low values of  $\gamma$ , the dominant layer is the first as it has the larger eigenvalue, see Fig. 2. Then, when surpassing  $\gamma^*$  (the point where  $\Lambda_1 = \Lambda_2$ ), there is a dominance change where the second layer has the largest eigenvalue. As we know the expression for the eigenvalue in a RR network, we can calculate the analytical form of  $\gamma^*$ . If we assume  $\Lambda_2 = k_\alpha \cdot (1 - (1 - \frac{1}{k_2})^{\gamma_2})$ , we obtain

$$\gamma^* = \frac{\ln\left(1 - \frac{\Lambda_1}{k_2}\right)}{\ln\left(1 - \frac{1}{k_2}\right)} \quad (10)$$

Using the numbers of the example,  $\gamma^* = 11.96$  where  $\Lambda_1 = k_1$ . This result is exact for a RR network. For an Erdős-Rényi network, we can approximate  $\gamma^*$ . See Fig. 2, the eigenvalue for the ER network behaves very similarly to the theoretical eigenvalue form for a RR network. Therefore, for low values of  $\gamma^*$ , we can approximate the eigenvalue of ER networks to the one for RR networks. For the layer with the  $\gamma \rightarrow \infty$ , we can not approximate the eigenvalue to the one of RR networks. Therefore, we can approximate  $\gamma^*$ . In the previous example,  $\gamma^* \approx 13.47$  for an ER network with  $\Lambda_1 \approx k_1 + 1$ .

This change of dominance is viewed in Fig. 3, where the inverse participation ratio for the second layer for low values of  $\gamma$  has the non-dominant form and, then, when  $\gamma^*$  is surpassed, it behaves as the dominant layer. We see how the dominance change behaves when changing  $\gamma$ . At first,  $IPR_2$  grows slowly, but when  $\gamma^*$  is almost reached, it increases rapidly. Then, when  $\gamma^*$  is surpassed, it stops suddenly to a constant value.

## V. SYSTEM DYNAMICS STUDY

In this section of the paper, we study Monte Carlo simulations for an ER two-layer network. We use a quasi-

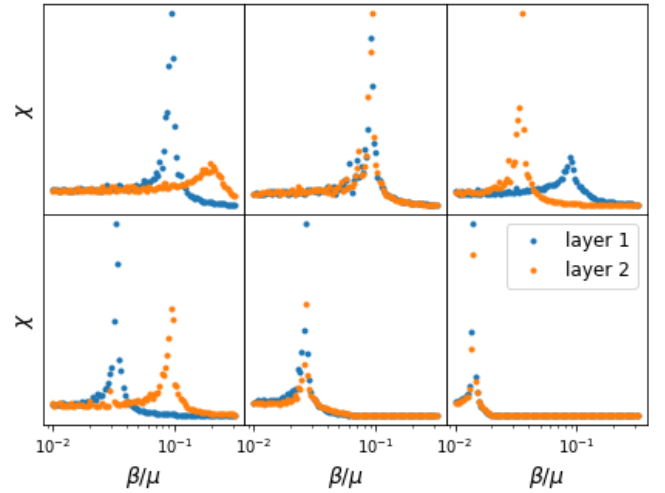


FIG. 4: The top panels are  $\chi$  in function of  $\beta/\mu$  with  $\eta = 0.1$ , the layer 1 with  $k_1 = 10$ ,  $\Lambda_1 \approx 11$  with  $\gamma_1 \rightarrow \infty$  and the layer 2 with  $k_2 = 30$ ,  $\Lambda_2 \approx 31$  and  $\gamma_2$  variable. Left to right, (i) first layer dominance regime with  $\gamma_2 = 5$ , (ii) near the dominance change with  $\gamma_2 = 13.5$ , (iii) second layer dominance regime with  $\gamma_2 = 100$ . The transition point is  $\gamma^* = 13.47$ . The bottom panels are  $\chi$  in function of  $\beta/\mu$  for different values of  $\eta$ . The layer 1 with  $k_1 = 30$ ,  $\Lambda_1 \approx 31$  and  $\gamma_1 = \infty$ . The layer 2 with  $k_2 = 10$ ,  $\Lambda_2 \approx 11$  and  $\gamma_2 = 10000$ . Left to right, (i4) localized regime with  $\eta = 0.01$ , (i5) near the localization change with  $\eta = 15$ , (i6) delocalized regime with  $\eta = 50$ . The transition point is  $p^* = 20$ . The code developed to get these results can be consulted in Ref. [6]

stationary algorithm [7] to avoid the absorbing state because if not the state would always reach it. We study dynamical behaviour for the different regime change viewed before, the localised to delocalised transition and the dominance transition. We simulate discrete time steps using the model described before where each node contacts its neighbour with certain probability and contacts himself on another layer. For a one layer simulation, we have a phase transition when the equilibrium state changes from being inactive to active while changing a structure variable of the system, in this case contact probability between layers. This transition can be studied with the modified susceptibility. It is defined

$$\chi = NM \frac{\langle \rho \rangle^2 - \langle \rho^2 \rangle}{\langle \rho \rangle}, \quad (11)$$

where  $\rho$  is the density when the stationary state is reached and  $NM$  is the dimension of the system. The susceptibility as a function of the structural parameter presents a diverging peak when the transition occurs. The peak position depends inversely to the largest eigenvalue of the system. Note that we are only interested in the position of the peaks therefore we do not care about the normalising factor. In a multiplex network we can study the density of each layer. In this scenario each

layer susceptibility has a peak when its transition occurs, however, only the dominant peak diverges.

We make different simulations changing network structural parameters to study the transitions analysed before in this paper. To analyse the localised-delocalised transitions we change  $\eta = \frac{\epsilon}{\beta}$  that equals  $p$  in the IPR study. To analyse the dominant-non dominant transition we change  $\gamma_2$  for the second layer.

In Fig. 4, we have represented different structures that characterise regimes that are valuable to study. The top panels study the dominance change. At  $\gamma_2^* > \gamma_2$  (i) the layer one dominates and has the diverging peak at  $\frac{\beta}{\mu} = \frac{1}{\Lambda_1}$  and layer two has its peak at  $\frac{\beta}{\mu} = \frac{1}{\Lambda_2}$ . Increasing  $\gamma_2$  increments  $\Lambda_2$  thus the peak moves, when  $\Lambda_1 = \Lambda_2$  both layers have a diverging peak at the same position (ii) and when  $\Lambda_1 < \Lambda_2$  (iii) the second layer peak diverge in  $\frac{\beta^*}{\mu} = \frac{1}{\Lambda_2}$ . The bottom panels study the localised to delocalised transition. The layer 1 always has the diverging peak at  $\frac{\beta}{\mu} = \frac{1}{\Lambda_1}$ . For low values of  $\eta$  (i4) the second layer has a peak in  $\frac{\beta}{\mu} = \frac{1}{\Lambda_2}$ , however, for bigger  $\eta$  values, this secondary peak disappears and reappears where the layer one peak locates, (i5) and (i6). When  $\eta \gg \eta^*$ , layers 1 and 2 behave equally and have a diverging peak.

## VI. CONCLUSIONS

In this paper, we have deduced a first order perturbation approximation for the parameter that characterizes the localised to delocalised transition for a social-contagion model on multiplex networks,  $p^*$ . The analytical expression have been obtained assuming a Random regular network but we show that it also accurately describes the transition point for Erdős-Renyi networks. With this approximation we also have obtained an analytical form for the non-dominant  $IPR_i$  when  $p < p^*$ . The numerical study of this parameters  $p^*$  and  $IPR_i$  was done in Ref. [5] but we have formalised an expression for them and also we have found an expression for their behaviour. We have also proven that scaling with  $p^*$  collapse  $IPR(p)$  for RR networks and ER networks.

Furthermore, we have studied a dominance change when varying  $\gamma$  for one layer, mentioned before in Ref. [3].

We have given an analytical expression for the transition point,  $\gamma^*$ , for RR networks and a precise approximation for Erdős-Renyi networks when  $\gamma^*$  is small.

Finally, we have corroborate our results by creating Monte Carlo quasi-stationary simulations to study dynamics of the multiplex system. By analysing different network structures we were able to observe the different dynamical behaviours of the transitions introduced in the paper.

However, an analytical form is needed to describe the IPR on the delocalised regime. In addition, a study of real networks that are well described for this multiplex social-contact model would be perfect to sum up this study. We hope that this paper helps a better understanding towards social networks and motivates other studies in this field.

## VII. APPENDIX

In the simulation, it is important to use a Quasi-stationary algorithm to describe the stochastic process properly. These processes change to a different state at each time step, however, there are absorbing states where the state can not evolve. The algorithm used dodges this state by saving previous states and changing randomly one for the absorbing state when it is reached. By doing this, our state has the same dynamics as a real quasi-stationary state except when a transition to the absorbing state is imminent [7]. The program is made in Python to use numpy and networks modules. We uploaded the code in a GitHub [6].

## Acknowledgments

I would like to give my deepest thanks to my advisor Dr. Emanuele Cozzo for his help, his guidance and his patience during this work. I would also like to thank my family for their support, with special mention to Marta Dominguez Navarro who has helped me a lot during the process.

---

[1] X. Zhang and A. A. Ghorbani, Information Processing Management **57**, 102025 (2020).  
[2] G. Ferraz de Arruda, F. Rodrigues, P. Rodríguez, E. Cozzo, and Y. Moreno, Journal of Complex Networks **6**, 215–242 (2018).  
[3] E. Cozzo, R. A. Baños, S. Meloni, and Y. Moreno, Physical Review E **88**, 10.1103/physreve.88.050801 (2013).  
[4] G. F. de Arruda, E. Cozzo, T. P. Peixoto, F. A. Rodrigues, and Y. Moreno, Physical Review X **7**, 10.1103/physrevx.7.011014 (2017).

[5] G. Ferraz de Arruda, J. A. Méndez-Bermúdez, F. A. Rodrigues, and Y. Moreno, Journal of Statistical Mechanics: Theory and Experiment **2020**, 103405 (2020).  
[6] J. Hernández-Tey, Github repository (2024), <https://github.com/JoanHTey/TFG>.  
[7] M. M. de Oliveira and R. Dickman, How to simulate the quasi-stationary state (2004), arXiv:cond-mat/0407797 [cond-mat.stat-mech] .